MedChemComm

CONCISE ARTICLE

View Article Online
View Journal | View Issue

Cite this: *Med. Chem. Commun.*, 2014, **5**, 219

Design and synthesis of a novel series of *N*,4-diphenylpyrimidin-2-amine derivatives as potent and selective PI3Kγ inhibitors

Hua-Lin Yang,† Fei Fang,† Chang-Po Zhao, Dong-Dong Li, Jing-Ran Li, Jian Sun, Qian-Ru Du and Hai-Liang Zhu*

Received 8th October 2013
Accepted 29th November 2013

DOI: 10.1039/c3md00301a

www.rsc.org/medchemcomm

Due to the increasing evidence linking the PI3Kγ pathway to various disease states, PI3Kγ is becoming an important target for cancer treatment. Herein we designed and synthesized a novel series of *N*,4-diphenylpyrimidin-2-amine derivatives with low CDOCKER_INTERACTION_ENERGY and then evaluated their PI3Kγ *in vitro* inhibitory activities and *in vitro* antiproliferation assays against four human cancer cells. Among the compounds we synthesized, compound **C8** (IC_{50} = 65 nM) demonstrated the most potent inhibitory activity against PI3Kγ kinase as well as at the cellular level, compared to the control drug **TG100713** (IC_{50} = 127 nM). Moreover, molecular docking analysis was also performed to determine possible binding modes between PI3Kγ and the target compounds.

Phosphoinositide 3-kinases (PI3Ks), the family of evolutionarily conserved lipid kinases, are categorized into class I, II, and III based on their subunit structure, regulation and substrate selectivity.[1,2] They all could catalyze phosphorylation of the 3-hydroxyl position of phosphatidylinositol 4,5-diphosphate (PIP2) to generate phosphatidylinositol 3,4,5-triphosphate (PIP3). PIP3 is known as a significant second intracellular messenger in the control of a diverse set of cellular processes, including cell growth, proliferation, differentiation, survival, intracellular trafficking and membrane ruffling.[2–6] The class IA (PI3Kα, PI3Kβ and PI3Kδ), as the most extensively studied of the three PI3K classes, is predominately activated by receptor tyrosine kinases and class IB (PI3Kγ) is activated by G-protein coupled receptors.[6,7] There is a regulatory subunit (p85) and an isoform-specific catalytic subunit (p110α, p110β and p110δ) to build up class IA, whereas PI3Kγ, the sole representative of class IB, consists of only one member: a p110γ catalytic subunit and a p101 regulatory subunit.[7–10] Three different subtypes of class IA PI3Ks (PI3Kα, PI3Kβ and PI3Kδ) are encoded by PIK3CA, PIK3CB and PIK3CD, respectively.[11]

In recent years, it has been widely reported that the deregulation of class I PI3Ks is responsible for cancer, inflammation, immune disorders, and cardiovascular diseases.[12] Moreover, PI3Kα and PI3Kβ, ubiquitously expressed in mammalian tissues, are involved in regulating tumor growth and proliferation, whereas PI3Kγ (mainly present in leukocytes) could be a viable approach for the treatment of a variety of inflammatory and cancer diseases.[13,14] As different subtypes of PI3Ks, the efforts to develop PI3K-targeted therapeutics have led to two paradigms: namely simultaneous inhibition of all PI3K isoforms (pan inhibition) and only one (isozyme selective).[9] Thanks to these efforts, there are a considerable number of compounds as anti-tumor agents now in clinic practice (Fig. 1). **LY294002**,[15] as the first PI3K inhibitor, is a pan inhibitor of PI3K kinase that binds reversibly to the ATP site and is also a commonly referenced compound in PI3K inhibition studies. **PIK-75**, **TGX221** (ref. 7) and **TG100713**[31] are isoform selective inhibitors, which exhibit potent, efficacious, antiangiogenic activity of PI3Kα, PI3Kβ and PI3Kγ, respectively.[16] Compared with isoform selective inhibitors, the pan inhibitors may cause some unexpected toxicities,[9] such as platelet aggregation and inhibition of immune responses. Based on these considerations, selective inhibition of PI3Ks has been considered as a comparative fashion for cancer treatment.

Given the linking of the PI3K pathway to various disease states, the class IA PI3Ks has been studied extensively as targets for the treatment of cancers and metabolic disorders.[13,14] However, there are only a handful of reports of PI3Kγ as the target for the treatment of inflammatory disorders and cancers in the previous literature, especially tumors. Recently, some papers linking the transforming functions of PI3Kγ to disrupt intercellular adhesion and promote cancer cell invasion have been published.[17–19] For example, PI3Kγ mediates Kaposi's sarcoma-associated herpesviruses GPCR-induced sarcomagenesis[20] and PI3Kγ activated by CXCL12 regulates tumor cell adhesion and invasion.[21] Therefore, based on these convincing pieces of evidence delineating a strong rationale in this

State Key Laboratory of Pharmaceutical Biotechnology, Nanjing University, Nanjing, 210093, P. R. China. E-mail: zhuhl@nju.edu.cn; Fax: +86-25-8359-2672; Tel: +86-25-8359-2572

† These authors contributed equally to this work.

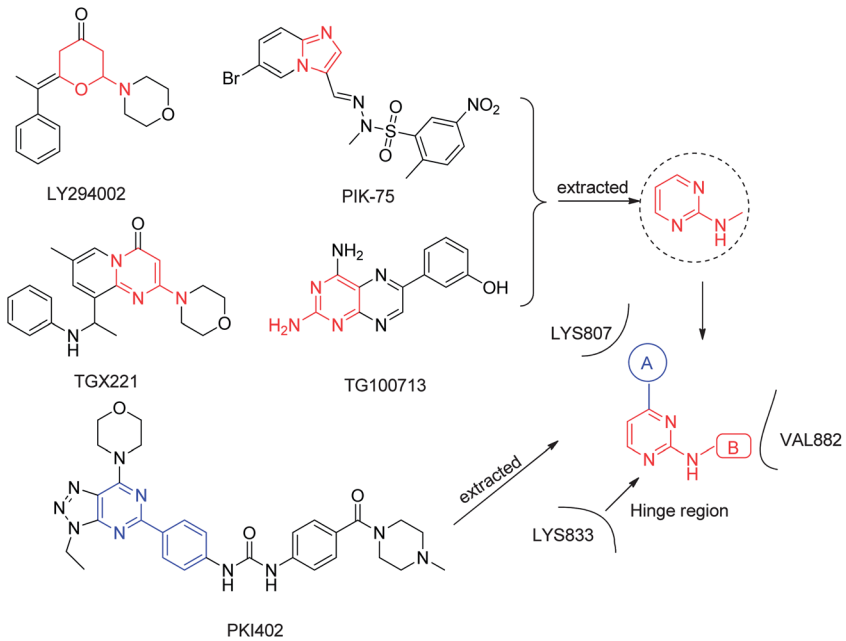

Fig. 1 Some known PI3K kinase inhibitors and design solution of novel *N*,4-diphenylpyrimidin-2-amine derivatives.

promising therapeutic area, it was decided to pursue PI3Kγ as a drug discovery target for cancer.

Pyrimidines were extensively explored and often used as central core structures[22] for the inhibitors of a wide range of kinases, such as Axl kinase,[23] phosphoinositide-3-kinase,[24] fibroblast growth factor receptor[25,26] and Janus tyrosine kinase.[27] Therefore, in order to develop more potent selective PI3Kγ inhibitors as anti-tumor agents, we attempted to use the pyrimidine core as the basic scaffold for designing the novel PI3Kγ inhibitors. As reported in previous studies, the exocyclic NH along with the pyrimidine core could form the classical bidentate hydrogen bond donor–acceptor interaction with the hinge region of the kinase,[28,29] and the pendant phenyl ring was identified as a suitable region for initial modification of the molecules.[16] Thus, the replacement of the aniline fragment at the 2-position of the pyrimidine ring would lead to alteration of these targets (Fig. 1). Moreover, pyrimidine, as a bioisostere of the quinoxaline ring moiety, shows some similarity in the structure to our referenced compound **TG100713** (from Selleck). Based on this, a series of novel *N*,4-diphenylpyrimidin-2-amine derivatives had been designed as the selective PI3Kγ inhibitors (Table 1) and the medicinal chemistry program was initiated to explore the SAR. Subsequently, in order to validate whether these small molecules could work on PI3Kγ and to verify the authenticity of the selected study only in PI3Kγ inhibitory activity at the same time, we have performed two groups of molecular dockings between these designed compounds and three protein–ligand complexes (as for PI3Kα, PDB code: **3HHM**; as for PI3Kβ, PDB code: **4G11**; as for PI3Kγ, PDB code: **1E8W**) retrieved from the RCSB Protein Data Bank (http://www.rcsb.org/pdb/home/home.do), by the means of the CDOCKER protocol[30] in the Accelrys Discovery Studio 3.5 suite.

After virtual screening, twenty-one *N*,4-diphenylpyrimidin-2-amine derivatives were synthesized for the study of anti-tumor activity. A general synthetic approach was developed to prepare these 2-aniline-pyrimidines that could be easily obtained by three steps in Scheme 1. These candidate compounds with *para* substituents on the E ring displayed low binding energy compared with the reference compound (**TG100713**), indicating that these compounds would be potential PI3Kγ inhibitors. To further

Table 1 Enzyme activities (IC_{50}, nM) of compounds **C1–C21** against human PI3Kγ, PI3Kα, PI3Kβ kinases, respectively

Compound	PI3Kγ IC_{50} (nM)	PI3Kα IC_{50} (nM)	PI3Kβ IC_{50} (nM)
C1	195	615	729
C2	167	552	603
C3	143	527	537
C4	235	738	839
C5	371	>1000	>1000
C6	334	880	>1000
C7	247	679	863
C8	65	341	373
C9	342	894	>1000
C10	357	>1000	977
C11	313	792	874
C12	302	914	946
C13	265	946	961
C14	231	591	673
C15	217	625	741
C16	154	503	573
C17	250	836	926
C18	274	813	851
C19	278	851	893
C20	386	953	938
C21	268	772	799
TG100713	127	165	215

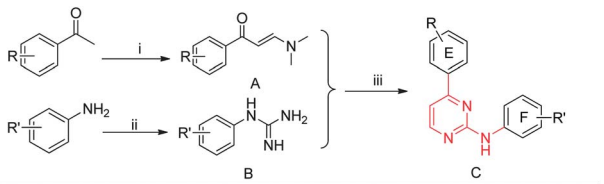

Compound	R	R'	Compound	R	R'
C1	4-methoxy	3-methoxy	**C12**	4-bromo	4-chloro
C2	4-methoxy	4-chloro	**C13**	4-bromo	4-nitro
C3	4-methoxy	4-nitro	**C14**	4-bromo	2,4-dichloro
C4	4-methoxy	2,4-dichloro	**C15**	3,4-dichloro	3- methoxy
C5	4-methyl	2,4-dichloro	**C16**	3,4-dichloro	4-nitro
C6	4-fluor	3-methoxy	**C17**	3,4-dichloro	2,4-dichloro
C7	4-fluor	4-nitro	**C18**	2,4-dichloro	3-methyl
C8	4-chloro	3,4,5-trimethoxy	**C19**	2,4-dichloro	3-methoxy
C9	4-bromo	3-methyl	**C20**	2,4-dichloro	4-nitro
C10	4-bromo	3-methoxy	**C21**	2,4-dichloro	2,4-dichloro
C11	4-bromo	2-isopropyl			

Scheme 1 Synthesis of compounds **C1–C21**. *Reagents and conditions*: (i) DMF-DMA/120 °C/16 h. (ii) Ar_2/EtOH/70% HNO_3/50% cyanamide/100 °C/16–18 h. (iii) Ar_2/NaOH/2-methoxyethanol/125 °C/22 h.

evaluate the selectivity for PI3Kγ, these candidates were also docked with PI3Kα (PDB ID: **3HHM**) and PI3Kβ (PDB ID: **4G11**), respectively. For better display and comparison with each other, these obtained results are plotted as a line–scatter graph presented in Fig. 2. It was composed of three trend lines: the black solid line that represented PI3Kγ; the blue solid line that represented PI3Kα; and the red solid line that represented PI3Kβ. The general trends of the corresponding CDOCKER_INTERACTION_ENERGY were similar against three enzymes, as shown in Fig. 2. For instance, the top compounds (**C9** and **C12**) and the bottom ones (**C3** and **C8**) were the same. However, the corresponding CDOCKER_INTERACTION_ENERGY of these compounds binding into PI3Kγ was obviously lower than that binding to PI3Kα and PI3Kβ. It was concluded that these candidates were promising to synthesize and evaluate as selective PI3Kγ inhibitors.

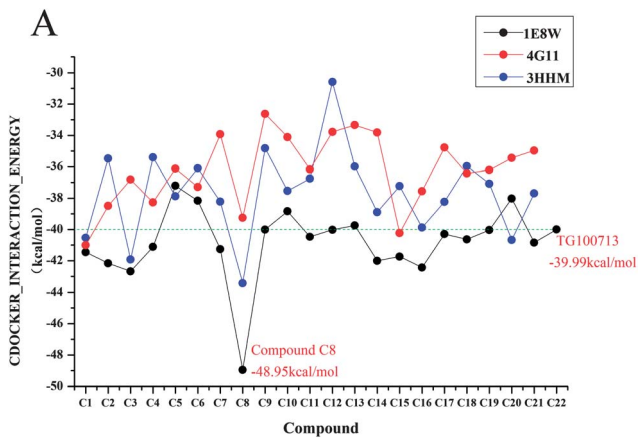

Fig. 2 The CDOCKER_INTERACTION_ENERGY (kcal mol^{-1}) obtained from the docking study of the targeted compounds by the CDOCKER protocol (Discovery Studio 3.5, Accelrys, Co. Ltd).

To get more direct insight into the binding mode of *N*,4-diphenylpyrimidin-2-amine derivatives and PI3Kγ, the binding model of 4-(4-chlorophenyl)-*N*-(3,4,5-trimethoxyphenyl)-pyrimidin-2-amine (compound **C8**) with the target protein structure (**1E8W**) is shown in Fig. 3. Visual inspection of the pose of compound **C8** in the PI3Kγ binding site revealed that this candidate PI3Kγ inhibitor was tightly embedded into the ATP binding pocket. The model also depicted that extensive hydrophobic interactions were formed between compound **C8** and residues **Ser 806, Lys 808, Pro 810, Ile 831, Asp 836, Ile 879, Glu 880, Asp 950** and **Asp 964** of the ATP-binding pocket of PI3Kγ

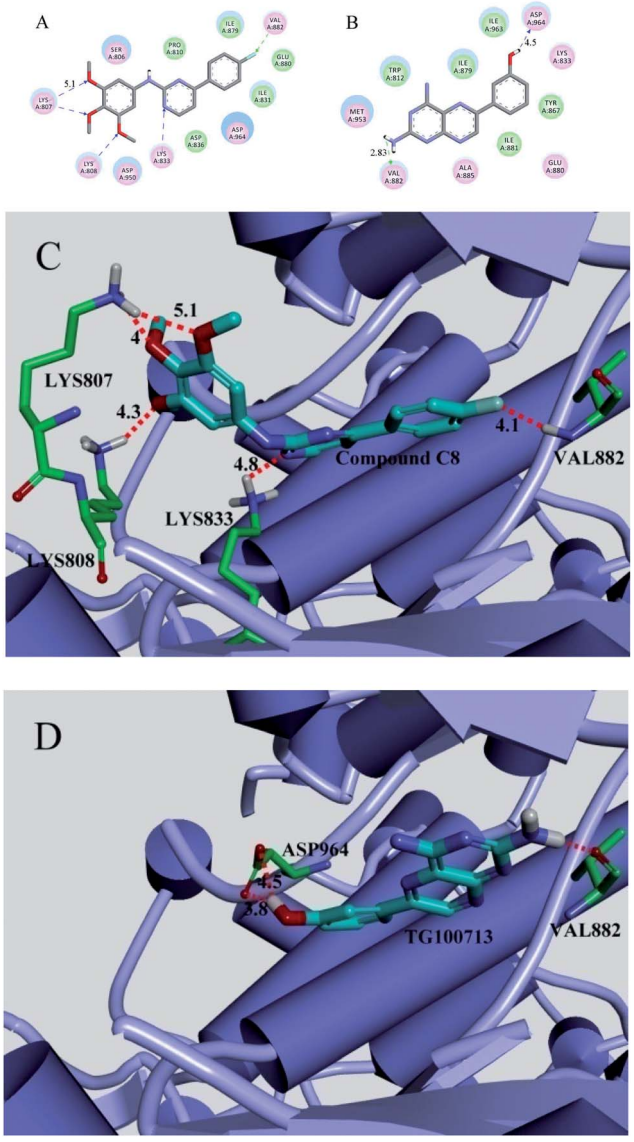

Fig. 3 The two kinds of binding modes between the active conformation of compound **C8**, **TG100713** (the reference drug) and the target protein PI3Kγ (PDB code: **1E8W**) provided by the CDOCKER protocol (Ligplus and Discovery Studio 3.5, Accelrys, Co. Ltd). (A) 2D molecular docking model of compound **C8** with **1E8W**. (B) 2D molecular docking model of **TG100713** with **1E8W**. (C) The 3D interaction map between compound **C8** and the PI3Kγ protein. (D) The 3D interaction map between **TG100713** and the PI3Kγ protein.

kinase (Fig. 3A). From Fig. 3C and D, there were only two H-bonds formed between the reference compound **TG100713** and **1E8W**, whereas five H-bonds were formed between compound **C8** and **1E8W**, inferring that the candidate was more tightly embedded into the ATP binding pocket than **TG100713**. Three H-bonds were formed between three methoxyl groups of the F ring and **Lys 807**, **Lys 808**, with their lengths 4 Å, 4.3 Å and 5.1 Å, respectively, as shown in Fig. 3C; another one, with its length 4.1 Å, was formed between *p*-Cl of the E ring and **Val 882**; the lengths 4 Å of H-bond was formed between N1 of the pyrimidine core and **Lys 883**, which was significant to bind the ATP-binding pocket of PI3Kγ kinase for all designed compounds. Based on these considerations, these results could provide a molecular level foundation for compound **C8** as the most potent PI3Kγ inhibitor.

Based on the docking results, herein we only focused on the replacement of substituents at 2-aniline and benzene ring at the 4-position of the pyrimidine skeleton. The synthesis of series **A** ((*E*)-3-(dimethylamino)-1-phenylprop-2-en-1-one) started from different substituted acetophenones by dissolving in DMF–DMA. Under Ar_2, substituted anilines were reacted with 50% cyanamide in EtOH to prepare the corresponding phenylguanidine derivatives **B**. Subsequently, a mixture of series **A**, series **B**, and NaOH in 2-methoxyethanol was heated at reflux to yield the target products **C** (Scheme 1).

Subsequently, all the synthesized compounds were evaluated for their inhibitory activities toward PI3Kγ, PI3Kα, and PI3Kβ, and the encouraging results are depicted as concentrations of IC_{50} in Table 1. As expected, most of the synthesized *N*,4-diphenylpyrimidin-2-amine derivatives showed moderate to potent inhibitory activities for these three target protein kinases, and the tendency of inhibition was roughly similar to our energy prediction. Moreover, most of these molecules also showed high selectivity over PI3Kα and PI3Kβ, compared with their IC_{50} in three target kinases from Table 1. Based on the obtained result, it was concluded that these synthesized compounds may have potential for further development as selective PI3Kγ inhibitors. In particular, compound **C8** of which the IC_{50} value could reach up to 65 nM, was a more potent PI3Kγ inhibitor than the referenced compound **TG100713** (IC_{50} = 127 nM), indicating that compound **C8** had a great opportunity as the new PI3Kγ selective inhibitor for cancer therapy.

According to the data shown in Table 1, it could be concluded that molecules with bulky substituents of the pyrimidine core could more easily bind to the active domain of PI3Kγ kinase. The inhibitory activity of compounds (**C1–C14**) with different *para* substituents on the E ring increased in the following order: 4-F < 4-Br < 4-methyl < 4-methoxy, inferring that those compounds with strong electron-donating groups performed better than those with electron-withdrawing substitutes. In addition, comparing all these potential inhibitors (especially among **C10**, **C15**, and **C19**), the disubstituents on the E ring were likely to be superior to monosubstitution inhibitors. In the light of steric and electronic factors, it could be noted that compounds with the same substituent on the phenyl E ring exhibited distinct kinase inhibitory activity due to different substituents which were introduced into the phenyl F ring. A comparison of the *para* substitution on the F ring demonstrated that a *para* electron-withdrawing group (compounds **C2**, **3**, **7**, **12**, and **13**) may have more slightly improved inhibitory activity than a methoxy or methyl group (compounds **C1**, **6**, **9**, and **10**), and it showed the most potent inhibitory activity when the *para* position was substituted by $-NO_2$ (compound **C3**, IC_{50} = 143 nM and compound **C13**, IC_{50} = 265 nM). Besides, the nitrogen at positions 1 and 3 of the pyrimidine ring could enhance the binding potency as PI3Kγ inhibitors. Based on the above results, these compounds in this series deserved further investigation.

These target compounds were also chosen to evaluate *in vitro* antiproliferation assays against four different human cancer cells (A549, MCF-7, HepG-2 and HeLa) as control for non-specific cytotoxicity. Interestingly, from the obtained results as listed in Table 2, compounds **C1–C21** almost showed moderate potent inhibitory activities against four cancer cells. And the representative compound **C8** exhibited the best inhibition activity with the IC_{50} values of 0.09 μM, 0.29 μM, 0.36 μM, and 3.15 μM, much better than those of the positive drug **TG100713** in some cell lines (HEPG2 and A549). In accordance with the PI3Kγ kinase assay, it was concluded that compounds **C8**, **C3**, **C16**, and **C4**, with the level of IC_{50} values in the low micromolar range, might be good candidates for further optimization. In

Table 2 *In vitro* anticancer activities (IC_{50}, μM) against four human tumor cell lines

	IC_{50} (μM)[a]			
Compound	HEPG2[b]	HeLa[b]	A549[b]	MCF-7[b]
C1	13.88	0.55	6.53	3.45
C2	4.50	0.31	20.89	0.81
C3	1.04	0.98	2.73	0.77
C4	0.19	23.03	7.33	4.17
C5	344.10	91.52	164.37	>1000
C6	127.64	145.01	35.91	412.45
C7	7.95	3.51	83.95	0.40
C8	0.09	0.29	0.36	3.15
C9	74.57	71.04	63.19	209.65
C10	148.05	152.71	82.66	278.17
C11	7.03	11.53	3.71	111.06
C12	47.48	36.68	6.11	4.18
C13	42.98	25.70	75.99	680.73
C14	0.72	1.08	3.78	2.49
C15	3.37	4.97	6	21.01
C16	0.5	1.84	0.72	3.51
C17	28.45	23.03	25.96	45.64
C18	13.15	7.66	18.45	248.63
C19	96.9	76.39	32.16	192.03
C20	99.33	167.93	119.38	192.45
C21	8.08	1.56	11.59	3.18
TG100713	0.82	0.15	0.49	1.03

[a] Antiproliferation activity was measured using the MTT assay. Values were determined from replicates of 6 wells from three independent experiments. [b] Cancer cells kindly supplied by the State Key Laboratory of Pharmaceutical Biotechnology, Nanjing University; HepG-2 (hepatocellular liver carcinoma cell line), MCF-7 (breast cancer), Hela (immortal cell line), and A549 (carcinomic human alveolar basal epithelial cell).

Table 3 IC_{50} data for compound **C8** against several-related kinases screened

Kinase	IC_{50} (μM)	Fold selectivity
PI3Kγ	0.065	—
EGFR	2.145	33
CDK2	18.782	289
PTK2	10.143	156
JAK2	21.513	331

short, these synthesized compounds played a role in inhibiting many tumor cell lines.

The kinase selectivity profile of this series was assessed, using compound **C8** as a representative. The obtained results (Table 3) presented their activity data depicted as IC_{50} values. Interestingly, compound **C8** showed moderate inhibitory activities for the majority of these target protein kinases, which belong to tyrosine and serine/threonine kinase. In addition, compound **C8** performed better as a PI3Kγ inhibitor than against other kinases. These results could provide sufficient evidence that compound **C8** could be selected as a potential PI3Kγ inhibitor and anti-tumor agent for further optimization.

For the sake of further assessing the inhibition of the target kinase by the synthesized compounds, an apoptosis experiment of compound **C8** was performed in the A549 cell line using Annexin-V and propium iodide (PI) double staining by flow cytometry. The uptake of Annexin V-PE notably increased, and the uptake of normal cells significantly decreased in a time-dependent manner. Finally the percentage of apoptotic cells from 5.47 ± 0.43% to 13.50 ± 0.79% was markedly elevated in a density-dependent manner at 48 h (Fig. 4). This is consistent with its good binding affinity to PI3Kγ and its potent activity in the inhibition of cell growth.

For further validation of the binding mode and the structural framework of the structure–activity relationship of these compounds, 3D-QSAR modeling was performed based on the docking results. The 3D-QSAR model was built by using the corresponding pIC_{50} values which were converted from the obtained IC_{50} (nM) values of PI3Kγ kinase inhibition and performed by built-in QSAR software of DS 3.5 (Discovery Studio 3.5, Accelrys, Co. Ltd). The way of this transformation was derived from an online calculator developed from an Indian medicinal chemistry lab (http://www.sanjeevslab.org/tools-IC50.html). The training and test sets were divided by the random diverse molecules method of DS 3.5, in which the test set accounts for 80% while the training set was set to 20%. 17 compounds were selected into training sets and the rest were in relative text sets. The results are presented in Table 4. During the development of 3D-QSAR modeling, one of the important steps was the determination of active conformation and alignment of molecules. The efficient solution of this model depended on a docking study and the reliability of a previous study about activity data. The alignment conformation of each molecule was the one with the lowest energy in the docked results of CDOCKER.

The 3D-QSAR model, generated from DS 3.5, defined the critical regions (steric or electrostatic) affecting the binding affinity, which was a PLS model built on 400 independent variables (conventional $r^2 = 0.94124$). The observed and predicted values and their residual values for the training set and test set molecules in the 3D-QSAR model are given in Table 4 and their graphical relationship is illustrated in Fig. 5, respectively. The plot of the observed IC_{50} *vs.* the predicted results

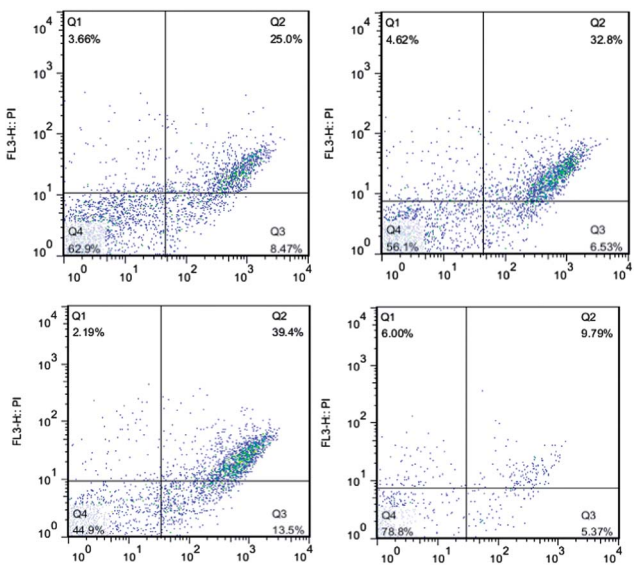

Fig. 4 Analysis of apoptosis induced by compound **C8** in the A549 cell line. Data represent the percentage of apoptotic cells. Cells treated with 1.0, 4.0, and 16.0 μM with compound **C8**.

Table 4 Experimental, predicted inhibitory activity of compounds **C1**–**C21**

	PI3Kγ kinase inhibition		
Compound	Actual pIC_{50}[b]	Predicted pIC_{50}	Residual error
C1	6.7100	6.7163	−0.0063
C2	6.7773	6.7808	−0.0035
C3	6.8447	6.8345	0.0102
C4	6.6289	6.6376	−0.0087
C5[a]	6.4306	6.6673	−0.2367
C6	6.4763	6.4712	0.0051
C7	6.6073	6.5979	0.0094
C8[a]	7.1871	7.1629	0.0242
C9	6.4660	6.4677	−0.0217
C10[a]	6.4473	6.5926	−0.1453
C11	6.5045	6.4923	0.0122
C12	6.5200	6.5557	−0.0357
C13	6.5768	6.6008	−0.0240
C14	6.6364	6.6233	0.0131
C15[a]	6.6635	6.5826	0.0809
C16	6.8125	6.8140	−0.0015
C17	6.6021	6.5951	0.0070
C18	6.5622	6.5371	0.0251
C19	6.5560	6.5531	0.0029
C20	6.4134	6.4014	0.0120
C21	6.5719	6.5675	0.0044

[a] Compounds were selected as the test sets while the rest were in the training sets. [b] The IC_{50} values of the compounds against PI3Kγ (Table 1) were converted into pIC_{50} values by using the online calculator (http://www.sanjeevslab.org/tools-IC50.html).

showed that this model has a good predictive power which could be used in the prediction of activity for new *N*,4-diphenylpyrimidin-2-amine derivatives as PI3Kγ inhibitors.

Also the molecules aligned with the iso-surfaces of the 3D-QSAR model coefficients on the electrostatic field region favorable (in blue) or unfavorable (red) and on the energy grids corresponding to the favorable (in green) or unfavorable (in yellow) steric effects for the PI3Kγ affinity are shown in Fig. 5B and C, respectively. It was widely acceptable that a better inhibitor based on the 3D-QSAR model should have strong van der Waals attraction in the green areas and a polar group in the blue electrostatic potential areas (which were dominant close to the skeleton). Several key features of the 3D-QSAR contour map are predicted to increase PI3Kγ inhibitor affinity: (1) a more positive environment all around the *para* position of ring E and the *meta* position of ring F (electronic study); (2) a more negative environment around the *para* position of ring F (electronic study); (3) less bulky *p*-substituent of the group of ring E and ring F (steric study); (4) more bulky group substituted in the *meta* position of ring F (steric study).

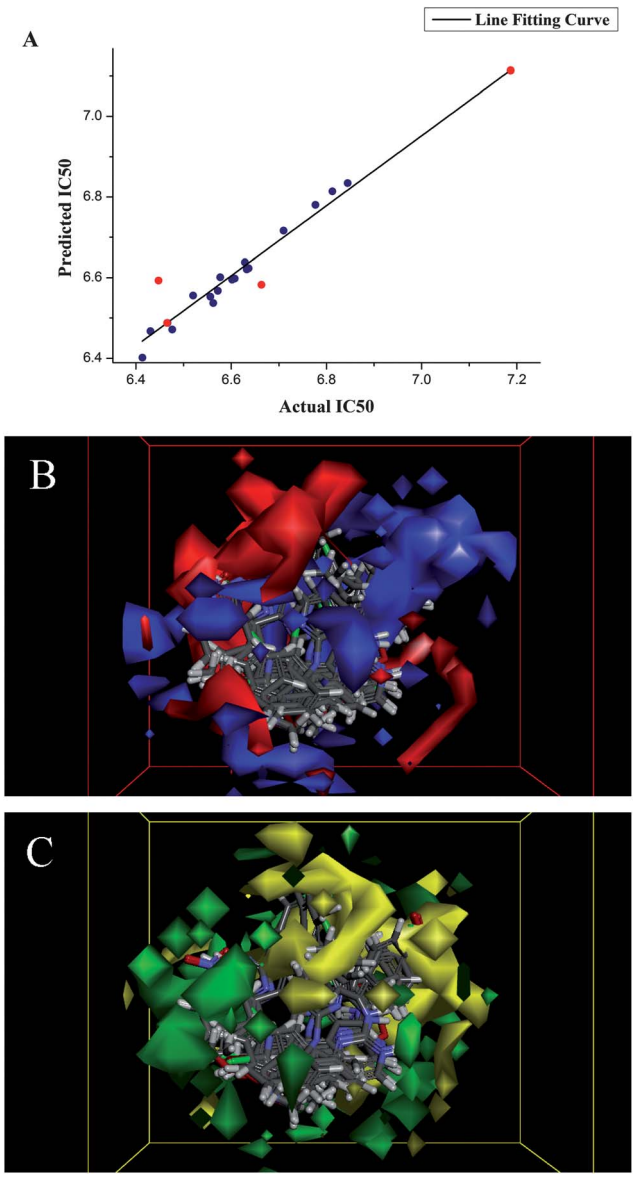

Fig. 5 (A) The predicted *versus* experimental pIC_{50} values for the inhibition of PI3Kγ (PDB: **1E8W**). (B) Isosurface of the 3D-QSAR model coefficients on electrostatic potential grids. The blue triangle mesh represents positive electrostatic potential and the red area represents negative electrostatic potential; (C) isosurface of the 3D-QSAR model on the steric effects. The green triangle mesh representation indicates that a larger volume is favorable; the yellow triangle mesh indicates the smaller one.

In summary, a series of *N*,4-diphenylpyrimidin-2-amine analogues have been synthesized based on the results of the virtual screening. These compounds showed modest potency and selectivity against PI3Kγ, with IC_{50} values up to nanomolar levels. Among these small molecules, the docking results indicated that compound **C8** could bind well inside the active site of PI3Kγ with the lowest CDOCKER_INTERACTION_ENERGY. Also, compound **C8** displayed the most potent anticancer activity against PI3Kγ (IC_{50} = 65 nM), being comparable with that of the positive control **TG100713** (IC_{50} = 127 nM). Moreover, the apoptotic cells with agent treatment accounted for 13.50%, as compared to 5.47% of apoptotic cells in the untreated control. This is consistent with its good binding affinity to PI3Kγ and its potent activity in the inhibition of cell growth. These results, along with the SAR analysis, were significant evidence to demonstrate that compound **C8** could be optimized as a potential selective PI3Kγ inhibitor in further studies.

Acknowledgements

This work was supported by the Jiangsu National Science Foundation (no. BK2009239) and the Fundamental Research Fund for the Central Universities (no. 1092020804).

References

1 D. A. Sabbah, N. A. Simms, M. G. Brattain, J. L. Vennerstrom and H. Z. Zhong, *Bioorg. Med. Chem. Lett.*, 2012, **22**, 876.
2 L. Bi, I. Okabe, D. Bernard, A. Wynshaw-Boris and R. Nussbaum, *J. Biol. Chem.*, 1999, **274**, 10963.
3 L. C. Cantley, *Science*, 2002, **296**, 1655–1657.
4 J. W. Leahy, C. A. Buhr, H. W. B. Johnson, B. Gyu, T. Baik, J. Cannoy, T. P. Forsyth, J. W. Jeong, M. S. Lee, S. Ma, K. Noson, L. Wang, M. Williams, J. M. Nuss, E. Brooks, P. Foster, L. Goon, N. Heald, C. Holst, C. Jaeger, S. Lam, J. Lougheed, L. Nguyen, A. Plonowski, J. Song, T. Stout, X. Wu, F. Michael, P. Yakes; Yu, W. T. Zhang, P. Lamb and O. Raeber, *J. Med. Chem.*, 2012, **55**, 5467.
5 D. Song, J. S. Yang, S. J. Kim, B. K. Kim, S. K. Park, M. Wonc, K. Lee, H. M. Kim, K. Y. Choi, K. Lee and G. Han, *Bioorg. Med. Chem. Lett.*, 2013, **21**, 788.
6 F. Giordanetto, A. Walberga, J. Cassel, S. Ghosal, M. Kossenjans, Z. Q. Yuan, X. P. Wang and L. F. Liang, *Bioorg. Med. Chem. Lett.*, 2012, **22**, 6665.
7 J. Kim, S. Hong and S. Hong, *Bioorg. Med. Chem. Lett.*, 2011, **21**, 6977.

8 J. D. Kendall, P. D. O'Connor, A. J. Marshall, R. Frédérick, E. S. Marshall, C. L. Lill, W. J. Lee, S. Kolekar, M. Chao, A. Malik, S. Yu, C. Chaussade, C. Buchanan, G. W. Rewcastle, B. C. Baguley, J. U. Flanagan, S. M. F. Jamieson, W. A. Denny and P. R. Shepherd, *Bioorg. Med. Chem.*, 2012, **20**, 69.

9 F. G. L. Turiso, Y. Shin, M. Brown, M. Cardozo, Y. Chen, D. Fong, X. L. Hao, X. He, K. Henne, Y. L. Hu, M. G. Johnson, T. Kohn, J. Lohman, H. J. McBride, L. R. McGee, J. C. Medina, D. Metz, K. Miner, D. Mohn, V. Pattaropong, J. Seganish, J. L. Simard, S. Wannberg, D. A. Whittington, G. Yu and T. D. Cushing, *J. Med. Chem.*, 2012, **55**, 7667.

10 C. Brock, M. Schaefer, H. P. Reusch, C. Czupalla, M. Michalke, K. Spicher, G. Schultz and B. Nurnberg, *J. Cell Biol.*, 2003, **160**, 89.

11 M. H. Norman, K. L. Andrews, Y. Y. Bo, S. K. Booker, S. Caenepeel, V. J. Cee, N. D. D Angelo, D. J. Freeman, B. J. Herberich, F. Hong, C. L. M. Jackson, J. Jiang, B. A. Lanman, L. Liu, J. D. McCarter, E. L. Mullady, N. Nishimura, L. H. Pettus, A. B. Reed, T. S. Miguel, A. L. Smith, M. M. Stec, S. Tadesse, A. Tasker, D. Aidasani, X. Zhu, R. Subramanian, N. A. Tamayo, L. Wang, D. A. Whittington, B. Wu, T. Wu, R. P. Wurz, K. Yang, L. Zalameda, N. Zhang and P. E. Hughes, *J. Med. Chem.*, 2012, **55**, 7796.

12 M. A. Crackower, G. Y. Oudit, I. Kozieradzki, R. Sarao, H. Sun, T. Sasaki, E. Hirsch, A. Suzuki, T. Shioi, J. Irie-Sasaki, R. Sah, H. M. Cheng, V. O. Rybin, G. Lembo, L. Fratta, A. J. Oliveira-dos-Santos, J. L. Benovic, C. R. Kahn, S. Izumo, S. F. Steinberg, M. P. Wymann, P. H. Backx and J. M. Penninger, *Cell*, 2002, **110**, 737.

13 T. B. Lanni Jr, K. L. Greene, C. N. Kolz, K. S. Para, M. Visnick, J. L. Mobley, D. T. Dudley, T. J. Baginski and M. B. Liimatta, *Bioorg. Med. Chem. Lett.*, 2007, **17**, 756.

14 T. Sasaki, J. Irie-Sasaki, R. G. Jones, A. J. Oliveria-dos-Santos, W. L. Stanford, B. Bolon, A. Wakeham, A. Itie, D. Bouchard, I. Kozieradzki, N. Joza, T. W. Mak, P. S. Ohashi, A. Suzuki and J. M. Penniger, *Science*, 2000, **287**, 1040.

15 C. J. Vlahos, W. F. Matter, K. Y. Hui and R. F. Brown, *J. Biol. Chem.*, 1994, **269**, 5241.

16 K. Bell, M. Sunose, K. Ellard, A. Cansfield, J. Taylor, W. Miller, N. Ramsden, G. Bergamini and G. Neubauer, *Bioorg. Med. Chem. Lett.*, 2012, **22**, 5257.

17 A. Ghigo, F. Damilano, L. Braccini and E. Hirsch, *BioEssays*, 2010, **32**, 185.

18 K. Reif, K. Okkenhaug, T. Sasaki, J. M. Penninger, B. Vanhaesebroeck and J. G. Cyster, *J. Immunol.*, 2004, **173**, 2236.

19 M. Laffargue, R. Calvez, P. Finan, A. Trifilieff, M. Barbier, F. Altruda, E. Hirsch and M. P. Wymann, *Immunity*, 2002, **16**, 441.

20 D. Martin, R. Galisteo, A. A. Molinolo, R. Wetzker, E. Hirsch and J. S. Gutkind, *Cancer Cell*, 2011, **19**, 805.

21 M. Monterrubio, M. Mellado, A. C. Carrera and J. M. R.-F. Rodriguez-Frade, *Biochem. Biophys. Res. Commun.*, 2009, **388**, 199.

22 A. Stella, K. Van Belle, S. De Jonghe, T. Louat, J. Herman, J. Rozenski, M. Waer and P. Herdewijn, *Bioorg. Med. Chem.*, 2013, **21**, 1209.

23 A. Mollard, S. L. Warner, L. T. Call, M. L. Wade, J. J. Bearss, A. Verma, S. Sharma, H. Vankayalapati and D. J. Bearss, *ACS Med. Chem. Lett.*, 2011, **2**, 907.

24 M. T. Burger, S. Pecchi, A. Wagman, Z. Ni, M. Knapp, T. Hendrickson, G. Atallah, K. Pfister, Y. Zhang and S. Bartulis, *ACS Med. Chem. Lett.*, 2011, **2**, 774.

25 V. Guagnano, P. Furet, C. Spanka, V. Bordas, M. Le Douget, C. Stamm, J. Brueggen, M. R. Jensen, C. Schnell and H. Schmid, *J. Med. Chem.*, 2011, **54**, 7066.

26 D. D. Li, F. Fang, J. R. Li, Q. R. Du, J. Sun, H. B. Hai-Bin Gong and H. L. Zhu, *Bioorg. Med. Chem. Lett.*, 2012, **22**, 5870.

27 J. J. Chen, K. D. Thakur, M. P. Clark, S. K. Laughlin, K. M. George, R. G. Bookland, J. R. Davis, E. J. Cabrera, V. Easwaran and B. De, *Bioorg. Med. Chem. Lett.*, 2006, **16**, 5633.

28 J.-L. L. Liao, *J. Med. Chem.*, 2007, **50**, 409.

29 A. C. Backes, B. Zech, B. Felber, B. Klebl and G. Müller, *Expert Opin. Drug Discovery*, 2008, **3**, 1427.

30 G. Wu, D. H. Robertson, C. R. Brooks and M. Vieth, *J. Comput. Chem.*, 2003, **24**, 1549.

31 J. Doukas, W. Wrasidlo and G. Noronha, *Proc. Natl. Acad. Sci. U. S. A.*, 2006, **52**, 19866.